A&A 395, 637–645 (2002)
DOI: 10.1051/0004-6361:20020977

Astronomy & Astrophysics

The complete far infrared spectroscopic survey of Herbig AeBe stars obtained by ISO-LWS

D. Lorenzetti[1], T. Giannini[1], B. Nisini[1], M. Benedettini[2], D. Elia[3], L. Campeggio[3], and F. Strafella[3]

[1] INAF – Osservatorio Astronomico di Roma, via Frascati 33, 00040 Monte Porzio, Italy
e-mail: teresa,bruni@coma.mporzio.astro.it
[2] Istituto di Fisica Spazio Interplanetario – CNR Area Ricerca Tor Vergata, via Fosso del Cavaliere, 00133 Roma, Italy
e-mail: milena@ifsi.rm.cnr.it
[3] Università degli Studi di Lecce – Dipartimento di Fisica, via Arnesano, 73100 Lecce, Italy
e-mail: eliad,campeggio,strafella@le.infn.it

Received 17 May 2002 / Accepted 28 June 2002

Abstract. The ISO-LWS archive has been systematically searched in order to obtain a complete far IR spectrophotometric survey of Herbig AeBe (HAEBE) stars. The investigated sample is constituted by 15 objects which, together with the 11 HAEBE we have published in two previous papers, represents about 25% of all the known HAEBE. This catalogue constitues an essential data-base in view of far IR forthcoming space missions (e.g. Herschel Space Observatory), whose scientific programs are now in the planning phase. The new sources are analysed following the same approach as in our previous papers and both differences and similarities are discussed in a coherent framework. The [OI] 63 μm and the [CII] 158 μm lines are observed in many of the investigated sources, while the [OI] 145 μm remains often undetected, due to its relative faintness. Molecular lines, in form of CO high-J rotational transitions are detected in only three cases and appear associated to local density peaks. A new class of ISO-LWS spectra of HAEBE emerges, constituted by objects without any detected gas feature either in emission or in absorption. Not unexpectedly, these HAEBE are isolated from molecular clouds and, as such, lack of the cold circumstellar material probed by far IR ionic and molecular transitions. By comparing line intensity ratios with model predictions we find that photodissociation caused by the stellar photons and active in a clumpy medium is likely the prevalent excitation mechanism for the far IR lines. Finally, an evolutionary trend is found according to which the contribution of the far IR line emission to the total emitted energy is less and less important with time.

Key words. stars: circumstellar matter – stars: pre-main sequence – infrared: ISM – ISM: lines and bands – infrared: stars

1. Introduction

Most of the recent studies on HAEBE stars deal with their circumstellar environments, where large scale phenomena (e.g. outflows, jets, heating and cooling of the circumstellar material) take place and IR excess emission, above that of the photosphere, originates. A significant fraction of the HAEBE's emitted power is released in the far IR range that is inaccessible from the ground (i.e. 45–200 μm) and that contains many emission lines which are unique tracers of the circumstellar gas physical conditions. The first spectrophotometric survey of HAEBE stars in this range has been obtained thanks to the ISO Long Wavelength Spectrometer (LWS) observations (Lorenzetti et al. 1999; Giannini et al. 1999; Papers I and II, respectively). These spectra show that [OI] 63 μm, 145 μm and [CII] 158 μm are by far the strongest emission lines so that they have been used to diagnose, as dominant excitation mechanism, the photodissociation supported by stellar more than interstellar photons. Molecular emission, in form of OH and CO transitions, with no evidence of water vapour emission, has been detected only toward those sources with high density ($n \gtrsim 10^6$ cm^{-3}) circumstellar material. Again, Photon Dissociated Regions (PDRs) models, allowing for some clumpiness (Burton et al. 1990), offer a satisfactory explanation for the molecular data, providing values for density (n) and radiation field (G_0) comparable to those derived from far IR ionic transitions.

Few other regions around HAEBE have been studied by means of ISO-LWS: the Cha II dark cloud (Nisini et al. 1996); the BD+40°4124 group (van den Ancker et al. 2000); the NGC 7023 region (Fuente et al. 2000); and He 3-672 (Malfait et al. 1998). All the results from these papers, dedicated to discuss specific properties of the investigated regions, are not in contrast with the above findings.

More recently the LWS spectra of six additional HAEBE stars (nearly all with A spectral types) have been investigated by Creech-Eakman et al. (2002). These authors provide an interpretation of the far IR continua in terms of passively heated,

Send offprint requests to: D. Lorenzetti,
e-mail: dloren@coma.mporzio.astro.it

flared, circumstellar disks. Their line analysis confirms our prior conclusions about the prevailing excitation mechanisms, but in almost all cases (5 out of 6) they report the unprecedented detection of HI and HeII recombination lines.

A large number of HAEBE stars has been also investigated with the ISO Short Wavelength Spectrometer (SWS) covering the 3–45 μm range (see: Waelkens et al. 1996; Malfait et al. 1998; Wesselius et al. 1996; van den Ancker et al. 2000; Thi et al. 2001; Benedettini et al. 1998, 2001; Meeus et al. 2001). SWS samples much more compact scales (from 10 to 20″) compared to the largest LWS field of view (~80″), therefore the two instruments investigate the circumstellar gas in substantially different conditions.

This paper aims to complete and extend our previous analysis to all the far IR spectra of HAEBE stars through an unbiased search from the ISO archive, in order to derive the far IR behaviour of HAEBE as a class. It is worthwhile noting that the same spectral range will be investigated at a much higher spectral ($\mathcal{R} \simeq 10^7$) and spatial (~9″) resolution with the instruments on board Herschel (Pilbratt 2001), hence the results of this spectroscopic survey can be considered as a useful database for planning future far IR observations.

2. Selected sample

We have searched the ISO archive (`http://www.iso.vilspa.esa.es/ida/index_us.html`) for LWS grating spectra of the objects listed in the most complete HAEBE stars compilation available to date (Thé et al. 1994, their Table 1). The archive search was simply made by centering a circular box on the HAEBE coordinates, whose size is the same of the LWS field of view (80″). We have found LWS spectra of 26 HAEBE out of the 108 catalogued objects. In Papers I and II we have presented the LWS data of 11 HAEBE along with two spectroscopic far IR maps (NGC 7129 and MWC 1080): these observations constituted part of the ISO guaranteed time program and, as such, they were obtained adopting a coherent strategy (e.g. selection criteria for sources; exposure times; ON and OFF source measurements for background evaluation). In the following we present LWS observations of the remaining 15 objects which belonged to different proposals which had different aims. Including these objects allows to more than double the so far available sample, thus achieving a significant coverage (~25%) of all the known HAEBE stars. It is remarkable that, despite the random selection criteria, the final sample spans a wide range of parameters such as the spectral type (from A8 to O7), the bolometric luminosity (from 5 to $1.3 \times 10^5\ L_\odot$), the circumstellar extinction (from 0.2 to 11 mag of visual extinction) and the associated outflow activity. The 15 new objects are listed in Table 1: the astrophysical parameters (distance, luminosity, A_V, etc.) have been taken by both Hipparcos (van den Ancker et al. 1998) and literature data; the parameter *r* following the IRAS name indicates whether the optical source is within the IRAS ellipse (e) or, otherwise, it gives the angular distance (in arcsec) between the optical and the IRAS peak; a flag near the source name signals that some results from the LWS spectrum of that source have been already presented in the literature according to the reference indicated. For these flagged sources we will emphasize here new line detections (if any) and additional aspects not commented in the previous papers.

3. Observations and data reduction

The observations were carried out with the Long Wavelength Spectrometer (LWS: Clegg et al. 1996, Swinyard et al. 1996) on board the Infrared Space Observatory (ISO: Kessler et al. 1996) in full grating scan mode (LWS01 AOT). This configuration provides coverage of the 43–196.7 μm range at a resolution $\mathcal{R} \sim 200$, with an instrumental beam size of ~80″. The spectra were oversampled by a factor of 4, were processed with the off-line pipeline (version 10) and reduced with the ISAP[1] (version 2.0). The flux calibration is based on observations of Uranus, resulting in an estimated accuracy of about 30% (Swinyard et al. 1996); the wavelength calibration accuracy is a small fraction (≈25%) of the resolution element, i.e. 0.07 μm in the range 43–90 μm and 0.15 μm in the range 90–196.7 μm. The steps of the data reduction are: (*i*) averaging the different spectral scans after removing the glitches due to the impact of cosmic rays; (*ii*) correcting the low-frequency fringes which result from interference along the optical axis with off axis emission (Swinyard et al. 1996). In Table 2 the observation parameters are given: Cols. 2 to 7 provide the coordinates of the pointed position; the total integration time (Col. 8) is obtained by means of a number of subsequent scans (Col. 9); finally the date and the orbit numbers are given in Cols. 10 and 11, respectively.

4. Results

The FIR spectra towards HAEBE stars consist of emission lines superimposed on a continuum. Discussion of both the continuum shape and a quantitative comparison with IRAS-PSC data, is reported in Elia et al. (2002). Figures 1–4 show the portions of the continuum subtracted spectra where lines with S/N ratio ≥3 have been detected; lines already presented in the previous literature are not replotted here.

The line analysis was performed on the defringed single detector spectra after subtracting a polynomial function which fitted the continuum and then using a single Gaussian function to fit the line profile. The errors on the line intensities correspond to a 1σ statistical uncertainties derived from the *rms* fluctuations adjacent to the line. The criteria adopted for line detection are the following: *i)* signal to noise ratio $S/N \geq 3$; *ii)* distance between observed and rest wavelength comparable to the wavelength calibration accuracy; *iii)* line width compatible with the nominal value of the relative detector (≈0.30 and 0.60 μm). The fluxes of the detected lines are given in Table 3.

By inspecting Table 3 we realize that, as expected, the spectra are dominated by the presence of fine structure lines of both [OI] and [CII] with additional ionic contributions

[1] The ISO Spectral Analysis Package is a joint development by the LWS and SWS Instrument teams and Data Center. Contributing Institutes are CESR, IAS, IPAC, MPE, RAL and SRON.

Table 1. Parameters of the investigated HAEBE.

Source	Spectral Type	L_{bol} ($L_\odot$)	A_V (mag)	Distance (pc)	IRAS name	r ($''$)	Other identifications
AB Aur[a,b]	B9-A0	48	0.50	140	04525+3028	e	BD+30°741 / HD31293 / MWC93
MWC 480[a]	A2/3	32	0.25	131	04555+2946	26	BD+29°774 / HD31648
HD 34282	A0V	4.8	0.59	160	05136-0951	e	BD-09°1110
MWC 758[a]	A3	22	0.22	200	05273+2517	e	BD+25°843 / HD36112
CQ Tau[a]	A8-F2	8	0.9	140	05328+2443	e	BD+24°873 / HD36910
MWC 137	B0	2.8×10^4	4.5	900	06158+1517	13	PN VV 42 / PK 195-00.1
He 3-672[c]	B9V	32	0.28	103	11312-6955	e	HD100546 / CPD-69°1557
He 3-741	A4	35	0.31	116	11575-7754	e	HD104237 / CPD-77°774
HD 141569	A0V	32	0.47	99	15473-0346	e	BD-03°3833
HD 142666	A8V	10.7	0.71	116	15537-2153	e	BD-21°4228 / CPD-21°6063
He 3-1141	A7V-F0	>30	0.56	>200	16038-2735	e	HD144432 / CD-27°10778
TY CrA[d]	B9	98	1.5	140	–		CPD-37°8450 / CD-37°13024
BD+40°4124 †[a,e]	B2V	3×10^3	3.0	1000	–		V1685 Cyg / He 3-1882 / MWC340
MWC 361[f]	B2/3V	8×10^3	1.92	430	–		HD200775 / BD+67°1283
LkHα233[a]	A7	100–150	2.6	800	–		V375 Lac / Mrk 914

Notes to the Table:
[a] Creech-Eakman et al. (2002); [b] Bouwman et al. (2000); [c] Malfait et al. (1998); [d] Corporon et al. (1999); [e] van den Ancker et al. (2000); [f] Fuente et al. (2000).
† the large LWS beam includes both LkHα 224 (an HAEBE star) and marginally LkHα 225 (an active embedded YSO) whose contributions can be separated only on SWS observations (van den Ancker et al. 2000).
r indicates the distance of the optical counterpart from the IRAS peak. Such distance is not given whenever the optical source lies within the IRAS uncertainty ellipse (e).

Table 2. Journal of observations.

Target	α(2000.0)			δ (2000.0)			t_{int}	n_{scan}	date	orbit
	h	m	s	°	′	″	(s)			
AB Aur	04	55	45.82	+30	33	05.3	2530	15	27 Feb 98	835
MWC 480	04	58	46.07	+29	50	37.3	2678	11	27 Feb 98	835
HD 34282	05	16	00.46	−09	48	33.8	2680	16	27 Mar 98	863
MWC 758	05	30	27.35	+25	19	58.0	2530	15	30 Mar 98	866
CQ Tau	05	35	58.40	+24	44	54.8	2080	12	15 Feb 98	823
MWC 137	06	18	44.83	+15	16	43.6	1124	8	13 Mar 98	849
He 3-672	11	33	25.67	−70	11	41.9	2228	4	29 Feb 96	104
He 3-741	12	00	05.07	−78	11	33.7	3340	7	22 Jun 97	584
HD 141569	15	49	57.60	−03	55	16.5	2228	13	04 Aug 97	627
HD 142666	15	56	40.08	−22	01	40.9	2206	13	12 Feb 97	454
He 3-1141	16	06	58.02	−27	43	10.0	2274	14	07 Sep 96	296
He 3-1141 OFF	16	06	55.93	−27	48	31.5	2274	13	07 Sep 96	296
TY CrA	19	01	40.68	−36	52	32.6	2112	5	29 Oct 96	348
BD+40°4124	20	20	28.30	+41	21	51.5	2080	12	23 Dec 97	768
MWC 361	21	01	36.91	+68	09	48.2	610	5	27 Oct 96	346
LkHα233	22	34	40.91	+40	40	04.6	2080	12	23 Dec 97	768

(i.e. [OIII]) detected only toward the small OB association BD+40°4124. Molecular emission, in form of high-J CO rotational transitions, occurs in those cases where the column density (A_V) is relatively large. Indeed the decreasing prevalence of molecular in favour of atomic line emission is a well recognized evolutionary trend, as already pointed out by Nisini et al. (2002), which is evident in going from the earliest phases of the protostellar evolution (Class 0 objects) toward Pre-Main Sequence stars (Class I/II objects). Molecular emission other than CO has been detected only in the spectrum associated to BD+40°4124. It presents a feature around 179 μm which can be attributed either to H_2O (179.53 μm) or to CH^+ (179.61 μm). Such emission could result from the contamination due to the shocked gas in the outflow of LkHα225 (Palla et al. 1995).

By comparing our results with those already published by other authors we find the same values within the given 1 or 1.5 σ error. Minor exceptions are: (*i*) CQ Tau: we failed in detecting the [OI] 63 μm line, found by Creech-Eakman et al. (2002) at a S/N level of about 5; (*ii*) BD+40°4124: conversely, here we report for the first time two more features at a significant level ($S/N \geq 5$), namely [NII] (122 μm) and H_2O or CH^+ (179 μm), not identified in the van den Ancker et al. (2000) spectrum. However, the relevant disagreement between our and previous results concerns the detection of HI (23–18),

(18–16), (20–17), (22–16) and HeII (23–21), (25–23) and (25–24) lines found by Creech-Eakman et al. (2002) in five out of six investigated objects. Their important claim has motivated us to perform a careful analysis of those spectral segments, but we can neither confirm their detections nor give any clue for the presence, at those wavelengths, of spectral features which could be assigned to transitions other than HI and HeII. We have been able to recognize only one emission feature in CQ Tau at 60.41 μm (with a $S/N \sim 2.5$), but we do not believe that helium recombination is plausible in view of the 10 000 K effective temperature of an isolated and late A-type star such as CQ Tau. Searching the available spectral line catalogues, a plenty of transitions corresponding to that wavelength are found, but no clear identification can be however attributed to the observed feature.

In principle, an OFF source spectrum should be taken at a suitable distance from the target in order to derive line intensities as uncontaminated as possible by the parent cloud emission. An OFF spectrum is available only for He 3-1141 in the presented sample of sources. To find a reasonable method for evaluating possible OFF contaminations at different wavelengths the following has been considered. From the sample presented in Paper I we know that [OI] 63 μm and [CII] 158 μm are the lines commonly detected in both the ON and OFF spectra. Because of the higher excitation temperature, the [OI] line is definitively brigther ON source, while the [CII] line tends to have comparable intensity between ON and OFF pointings for the low luminosity sources, corresponding to low flux levels of 2–5$\times 10^{-20}$ W cm^{-2}. This fact has been also confirmed by the OFF measurement of He 3-1141, where the $[\mathrm{CII}]_{\mathrm{OFF}}$ flux is $4.1 \pm 0.5 \times 10^{-20}$ W cm^{-2}, about the same value of the ON flux.

Creech-Eakman et al. (2002) performed an analysis of the background contamination around HAEBE stars using COBE, ISOPHOT and IRAS data reaching slightly different results. They found for all their stars (with the exception of BD+40°4124) a contamination level in the $100 < \lambda < 240$ μm range less than 0.7×10^{-20} W cm^{-2} in the LWS spectral resolution element (this value is about 13 times larger for BD+40°4124). As a consequence, they did not apply any background correction to their data. Although neglecting or not the background contributions have minor implications on deriving the overall properties of the HAEBE stars, nevertheless we note how their estimate (when checked on the only available case) attributes to the [CII] diffuse emission a value more than a factor of five lower than the detected value.

Based on the above arguments: (*i*) a value of $2-5 \times 10^{-20}$ W cm^{-2} will be adopted in the following as the background contribution to the [CII] emission in regions around objects with A spectral type; (*ii*) a reduction by a factor of two will be applied to the high [CII] flux levels; (*iii*) no correction at all will be done to the [OI] emission. Only the case of BD+40°4124 should be considered with some caveat.

The spectroscopic data given in Table 3 indicate that a subclass of HAEBE stars exists constituted by objects which show either no far IR emission line (MWC 480, HD 141569 and He 3-1141) or only small [CII] contributions marginally above the ubiquitous interstellar value (HD 34282, MWC 758, CQ Tau and HD 142666). The above mentioned HAEBE have an A-spectral type and an A_V value less than unity, conditions which both inhibit the excitation of the cold circumstellar material by stellar photons. Basically these objects are the least luminous ones among our sample, having all $L_{\mathrm{bol}} \lesssim 30\ L_{\odot}$ (see Table 1). From an observational point of view this limit represents an important prescription for selecting targets of future space missions; the implications of this threshold will be discussed in the next section.

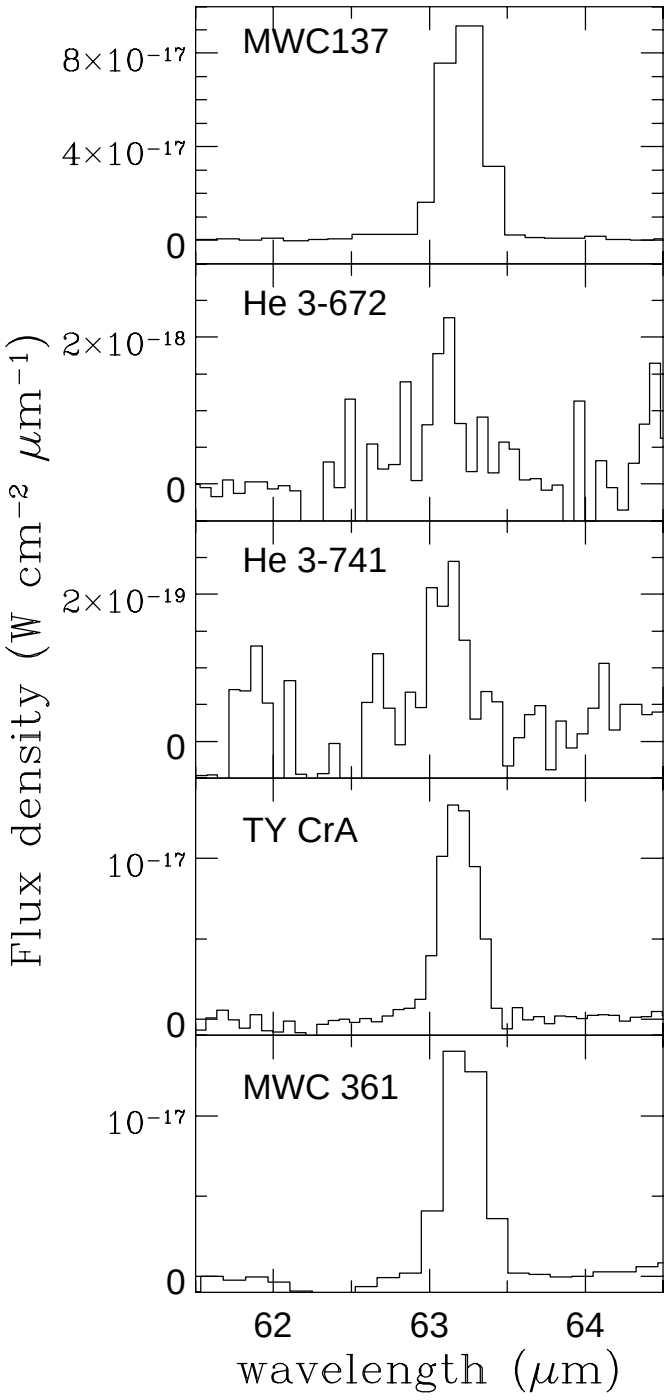

Fig. 1. Continuum subtracted LWS spectra of the investigated HAEBE stars: selected ranges containing the [OI] 63 μm line. Lines already presented in the previous literature are not re-depicted here.

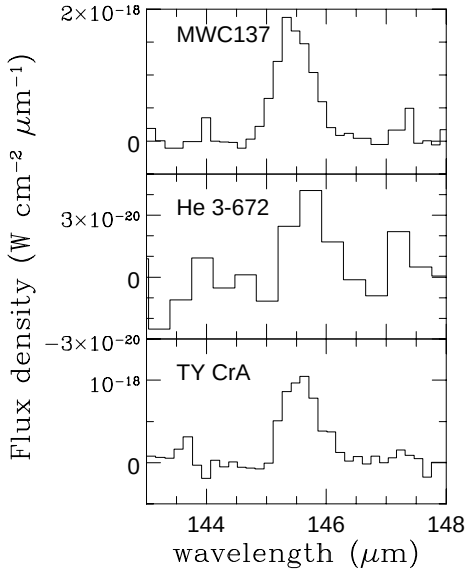

Fig. 2. As in Fig. 1 for the [OI] 145 μm line. The spectrum of He 3-672 has been re-binned at a lower resolution in order to increase the signal to noise ratio.

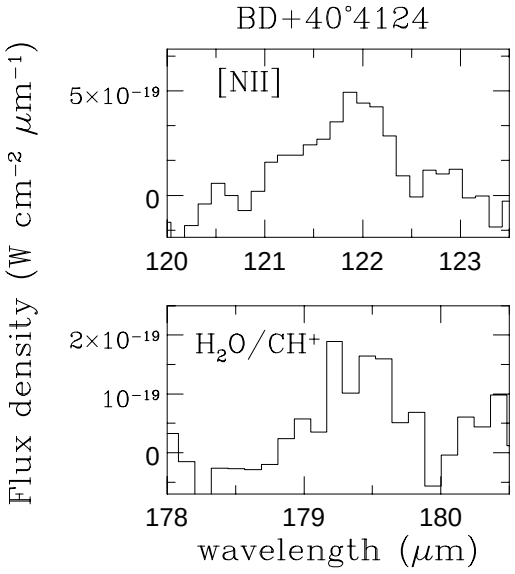

Fig. 4. As in Fig. 1 for the [NII] 122 μm and 179 μm emission feature (attributable to H_2O or CH^+). Both lines are detected for the first time in BD+40°4124.

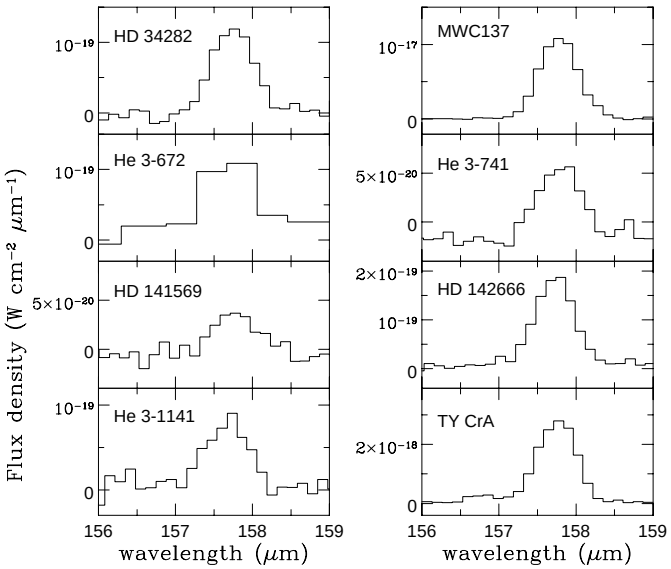

Fig. 3. As in Fig. 1 for the [CII] 158μm line. The spectrum of He 3-672 has been re-binned at a lower resolution in order to increase the signal to noise ratio.

5. Discussion

5.1. [OI] and [CII] lines

The [OI] 63, 145 μm and [CII] 158 μm are the strongest features observed and have been used in Paper I as a diagnostic of the excitation mechanism and then of the physical conditions. Here we intend to follow the same method, namely to check whether or not the HAEBE of the present sample behave as the objects considered in Paper I. Line ratios and corresponding errors of the stars presented here are indicated in Fig. 5, where those already presented in Paper I are also reported for completeness but without any flag.

The observed line intensity ratios are superimposed in Fig. 5 on a grid of photodissociation models (Kaufman et al. 1999). The substantial difference between line intensity predictions of this model and those of other PDR models (e.g. Tielens & Hollenbach 1985) is the inclusion of an additional heating: the ejection of photoelectrons from PAH and small grains. These latter are essential component of the HAEBE close environments, as demonstrated by many dedicated observations (see e.g. Meeus et al. (2001) and references therein). The extra heating source is essential because for a given value of density (n) and radiation field (G_o), this model predicts increased OI and CII column densities, thus allowing to move at lower n and G_o the transition point between CII dominated and OI dominated cooling. The location of the data points in Fig. 5, although in two cases (identified by the letters c and e) not perfectly coincident with the model grid, gives further support to our previous interpretation in favour of phodissociation as dominating mechanism for far IR line excitation. Our hypothesis about the existence, around the HAEBE stars, of a PDR originated by stellar rather than interstellar FUV photons has received further support by the correlation between [CII] 158 μm luminosity vs. the bolometric luminosity of the central source shown in Fig. 5 of Paper I. With reference to that plot, we note that the values (L_{bol}, $L_{[CII]}$) of the new sources investigated here are perfectly aligned along the already presented relationship.

Alternative models do not seem so much promising: J-shock models (e.g. Hollenbach & McKee 1989) can be ruled out, since they predict substantially different line ratios whose intersection with our PDR plane is indicated in Fig. 5 as the hatched area at the top right corner. Since a considerable fraction of the HAEBE is expected to drive molecular outflows, the role of non dissociative C-shocks (e.g. Draine et al. 1983) has been discussed in more detail in Paper I, where we conclude that possible contributions of C-shocks to the far IR emission

Table 3. Line intensities of HAEBE stars.

Source	λ_{obs} (μm)	Identification	$F \pm \Delta F$
AB Aur	63.18	[OI] $^3P_1$–$^3P_2$	$8 \pm 3^{a,b}$
	157.77	[CII] $^2P_{3/2}$–$^2P_{1/2}$	8.7 ± 0.7
MWC 480	157.77	[CII] $^2P_{3/2}$–$^2P_{1/2}$	5.5 ± 0.4
HD 34282	157.74	[CII] $^2P_{3/2}$–$^2P_{1/2}$	9.8 ± 0.4
MWC 758	157.79	[CII] $^2P_{3/2}$–$^2P_{1/2}$	12.3 ± 0.6
CQ Tau	157.75	[CII] $^2P_{3/2}$–$^2P_{1/2}$	15.3 ± 0.6
MWC 137	63.20	[OI] $^3P_1$–$^3P_2$	3467 ± 13
	145.46	[OI] $^3P_0$–$^3P_1$	136 ± 4
	157.77	[CII] $^2P_{3/2}$–$^2P_{1/2}$	696 ± 4
He 3-672	63.13	[OI] $^3P_1$–$^3P_0$	66 ± 13
	145.70[c]	[OI] $^3P_1$–$^3P_0$	3.2 ± 0.8
	157.72	[CII] $^2P_{3/2}$–$^2P_{1/2}$	11 ± 1
He 3-741	63.10[c]	[OI] $^3P_1$–$^3P_2$	6 ± 1
	157.79	[CII] $^2P_{3/2}$–$^2P_{1/2}$	4.4 ± 0.4
HD 141569	157.75	[CII] $^2P_{3/2}$–$^2P_{1/2}$	3.8 ± 0.5
HD 142666	157.72	[CII] $^2P_{3/2}$–$^2P_{1/2}$	10.7 ± 0.5
He 3-1141	157.72	[CII] $^2P_{3/2}$–$^2P_{1/2}$	4.4 ± 0.3
TY CrA	63.18	[OI] $^3P_1$–$^3P_2$	405 ± 14
	145.57	[OI] $^3P_0$–$^3P_1$	79.0 ± 0.6
	153.11[c]	CO 17–16	7 ± 3^a
	157.75	[CII] $^2P_{3/2}$–$^2P_{1/2}$	173 ± 3
	163.00[c]	CO 16–15	6 ± 3^a
BD+40°4124	51.84	[OIII] $^3P_2$–$^3P_1$	53 ± 8
	63.17	[OI] $^3P_1$–$^3P_2$	736 ± 7
	88.39	[OIII] $^3P_1$–$^3P_0$	79 ± 7
	121.91	[NII] $^3P_2$–$^3P_1$	35 ± 5^b
	145.50	[OI] $^3P_0$–$^3P_1$	51 ± 4
	153.36	CO 17–16	13 ± 4
	157.73	[CII] $^2P_{3/2}$–$^2P_{1/2}$	560 ± 4
	162.83	CO 16–15	21 ± 3
	173.52	CO 15–14	27 ± 4
	179.44	H_2O 2_{12}–1_{01}	16 ± 4
		CH^+ 2–1	
	185.87	CO 14–13	13 ± 3
MWC361	63.21	[OI] $^3P_1$–$^3P_2$	504 ± 15
	145.63	[OI] $^3P_0$–$^3P_1$	65 ± 1
	157.76	[CII] $^2P_{3/2}$–$^2P_{1/2}$	285 ± 3
	162.65[c]	CO 16–15	7 ± 3^a
LkHα233	63.20	[OI] $^3P_1$–$^3P_2$	19 ± 3
	145.60	[OI] $^3P_0$–$^3P_1$	2.9 ± 0.9
	157.74	[CII] $^2P_{3/2}$–$^2P_{1/2}$	45.4 ± 0.9

Notes: [a] S/N between 2 and 3; [b] $FWHM$ smaller or larger than instrumental; [c] distance between observed and rest wavelength marginally exceeding the resolution element. Fluxes are expressed in 10^{-20} W cm^{-2}.

lines cannot be ruled out, but such mechanism can be considered as the main responsible for the gas excitation just in a narrow region of the parameter space (shock speed, magnetic field, pre-shock density).

The plot depicted in Fig. 5 has to be regarded as a useful tool to assess the prevailing excitation mechanism for the HAEBE class of objects, but cannot be used for finely deriving the physical parameters of the associated PDRs. Even in those cases where the small errors would formally allow such a derivation, the values are to be considered with some caution. Possible self-absorption of [OI] 63 μm or thickness effects on both the [OI] lines discussed below (Sect. 5.4), tend to make uncertain the definition of the PDR parameters. In the next section a more reliable diagnostic, based also on molecular line emission, will be discussed.

5.2. Molecular emission

Out of the 15 considered HAEBE, we found molecular emission in form of CO rotational transitions in three objects: TY CrA, BD+40°4124 and MWC 361; hence the detection rate of molecular emission estimated on the overall sample is about 25% (6 out 26 objects). Although molecular lines are usually weak (see Table 3 and Paper II), we do not believe the lack of detection in other sources is due only to an instrumental sensitivity limit, but it is also related to an intrinsic property of the circumstellar environment, namely the existence or not of some compact density peaks near the source where the column density is expected to substantially increase. This occurrence has been already discussed in Paper II and our aim is to check this point on the three objects considered here.

To do that we have calculated the CO luminosity starting from the detected rotational lines, using our Large Velocity Gradient (LVG) code (see Paper II for details) to solve the equations of the statistical equilibrium for the level population. The total CO luminosity (L_{CO}) is derived by summing up all the intensities predicted by the model, while the associated uncertainty of about 30% stems from the spread among the best 30 models. Once L_{CO} is obtained for each source, we have plotted $L_{CO}/L_{[OI]145}$ vs. $L_{CO}/L_{[CII]}$ in Fig. 6 along with the clumpy PDR model predictions by Burton et al. (1990). This plot offers the advantage of providing a diagnostic of the physical conditions by means of both atomic and molecular line emission; moreover it uses transitions not affected (as the [OI] 63 μm) by possible self-absorption problems. We note that the reduction or not (by a factor of two) the flux of the [CII] 158 μm line to account for the background contribution (see Sect. 4), does not significantly alter the data points in Fig. 6. These circumstances make the plot in Fig. 6 more reliable than that in Fig. 5. In Fig. 6 all the HAEBE showing molecular emission are depicted, although three of them (R CrA, IRAS 12496 and LkHα 234) were discussed in Paper II. The newly considered objects (TY CrA, BD+40°4124 and MWC 361) trace densities of the order of 10^6 cm^{-3} or less and G_o between 10^3 and 10^4, confirming the association between molecular emission and high density condensations. Support to this finding comes from independent observations: according to CO data in the CrA region, the column density maximum is close to the position of TY CrA where $n > 10^4$ cm^{-3} (Harju et al. 1993); clumpy

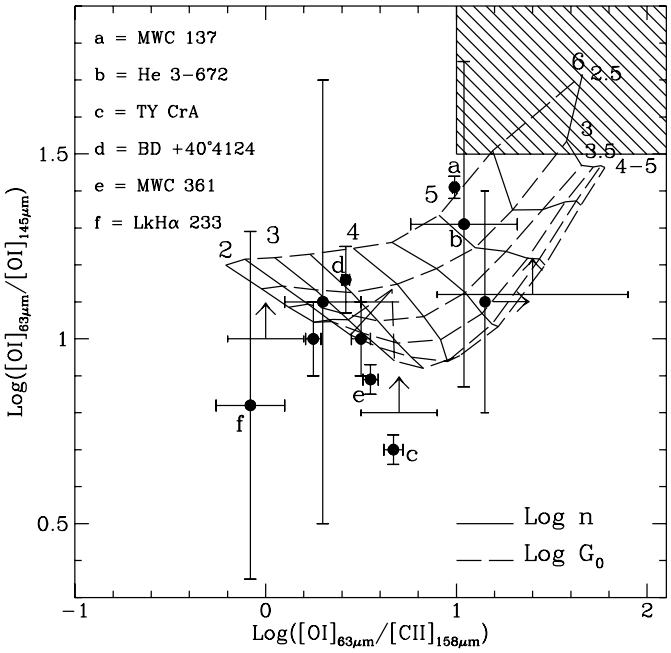

Fig. 5. Observed line ratios superimposed to PDR models by Kaufman et al. (1999). The hatched area identifies the locus pertaining to the J-shock model predictions.

photodissociation regions (PDRs) with high density filaments ($n \sim 10^5$–10^6 cm^{-3}) are expected to be immersed in a more diffuse medium around MWC 361 (Fuente et al. 2000); a clumpy PDR (with $n \sim 10^6$ cm^{-3}) is proposed by van den Ancker et al. (2000) as the unique alternative to account for their observations of the BD+40°4124 region. If molecular emission originates close to density peaks it could be associated, rather than to the HAEBE itself, to a nearby and more embedded companion of the kind that has sometimes been discovered in HAEBE neighbourhoods (e.g. Font et al. 2001).

Apart from photodissociation, a deeper discussion on the remaining alternatives is done in Paper II. Here we remember that molecular emission can also occur in *C*- or *J*-shocks. However, *J*-shocks at low values of the pre-shock density ($n_0 \simeq 10^4$ cm^{-3}) predict $L_{[OI]}/L_{CO} \gg 1$, while we have for TY CrA, BD+40°4124 and MWC 361 quite low values for the $L_{[OI]}/L_{CO}$ ratio (0.7, 0.2, 0.3, respectively). According to both *C*-shocks and *J*-shocks at high values of the pre-shock density ($n_0 \simeq 10^6$ cm^{-3}), water should be the main coolant with a predicted cooling ratio $L_{H_2O}/L_{CO} \sim 10$, clearly in contrast with the absence of water emission in all the 26 HAEBE. In conclusion, the combined diagnostic provided by fine structure and molecular line emission tends to favour the photodissociation mechanism possibly operating in a clumpy medium.

5.3. Ionised lines

Fine structure lines from different ions are detected, among the objects presented here, only toward BD+40°4124 in form of [OIII] 52 and 88 μm and [NII] 122 μm transitions. This circumstance is not unexpected since this source belongs to the only OB association among our sample. Previously, van den Ancker et al. (2000), by using the intensity ratio of the [OIII] lines, found they are formed in a HII region with an electron density $n_e = 0.6$–2.2×10^2 cm^{-3}. Their paper provides a deep study of the BD+40°4124 group, also including the nearby objects and the relative SWS observations. Here we have also detected the [NII] 122 μm line which is a typical tracer of low ionisation and low density material. From the ratio [CII]158 μm/[NII]122 μm $\simeq$ 16, we derive, by using the Petuchowsky & Bennet model (1993), a lower value of $n_e = 25$ cm^{-3}, which indicates the presence of an electron density gradient moving away from the central object.

5.4. About the ratio [OI]63 μm/[OI]145 μm

Considering all the 26 HAEBE we note that, when the 145 μm line is detected, the [OI]63 μm/[OI]145 μm line ratios range between 2 and 10 with few exceptions at larger values (see Paper I and Fig. 5). Conversely, the models either simply based on density and temperature conditions (e.g. Watson 1984) or oriented to specific excitation mechanisms (PDR, *J*-, *C*-shocks), all predict larger values of this ratio typically in the range 20–100 or more; in this framework, the observed values represent systematically quite marginal cases. The unconsistency between model predictions and observed [OI] line ratios is emphasized by independent evidences coming from all the authors who have studied star forming regions with ISO-LWS data (e.g. Fuente et al. 2000; Liseau et al. 1999; Saraceno et al. 1998). The only exception is represented by the class of the Herbig-Haro objects, whose observed ratios are between 15 and 25 (e.g. Molinari et al. 2001; Nisini et al. 1996). In Paper I we have explained the low ratios as due to the presence of foreground cold OI responsible for an absorption at 63 μm and thus producing a net decrease of the 63 μm flux emitted by the source. But $A_V \geq 5$ mag is required to justify such an absorption, therefore this explanation cannot be extended to the objects presented in this paper because those having 63/145 ratio less than 10 have all $A_V < 2.5$ mag. A possible interpretation for the recurrent low values could be related to the optical depth of both lines. Values between 2 and 10 can be obtained in a gas with a temperature between 100 and 500 K, if both lines are optically thick (see e.g. Fig. 2 of Tielens & Hollenbach 1985). By assuming an oxygen abundance $X(O)/X(H) = 3.2\times10^{-4}$ (Meyer et al. 1998) with all the oxygen in the OI form and a dispersion velocity of 2 km s^{-1}, we obtain that the required column densities to make the $\tau_{63\ \mu m}, \tau_{145\ \mu m} \geq 1$ are 3.3×10^{22} and 2.2×10^{22} cm^{-2} at 100 and 500 K, respectively. These values correspond to $A_V = 17$ and 11 mag, by adopting the total-to-selective extinction ratio $R = 3$. Since $R = 5$ seems more appropriate for grains around HAEBE (Pezzuto et al. 1997), the A_V values move in the range 27–18 mag. These conditions (temperatures of about 100–500 K and high optical depths) are typical of compact structures such as disks or clumps around the central object (Burton et al. 1990). A rough estimate of the size *l* of the emitting region, can be derived from the ratio between the column and the volume density ($l \simeq N/n$ cm), if homogeneity and spherical symmetry are assumed as for the circumstellar environment. By adopting the clump densities derived from Fig. 6

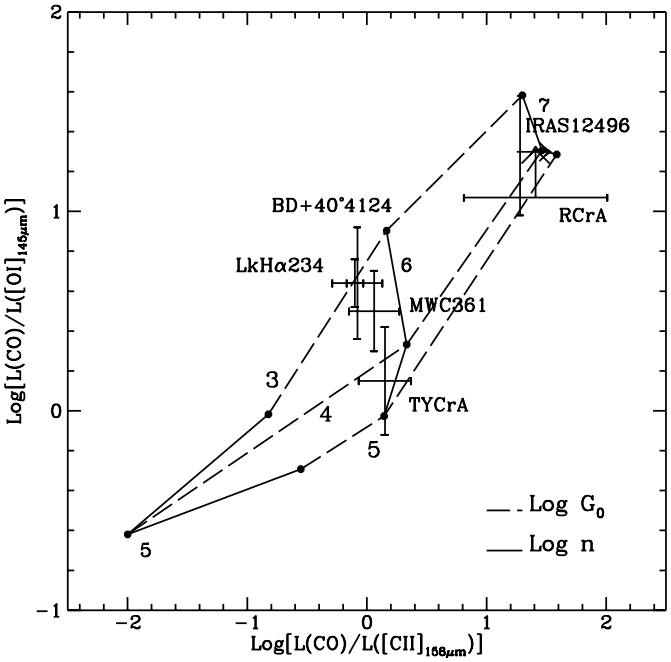

Fig. 6. Observed ratios between molecular CO lines and fine structure [OI] 145 μm and [CII] 158 μm superimposed on clumpy PDR models.

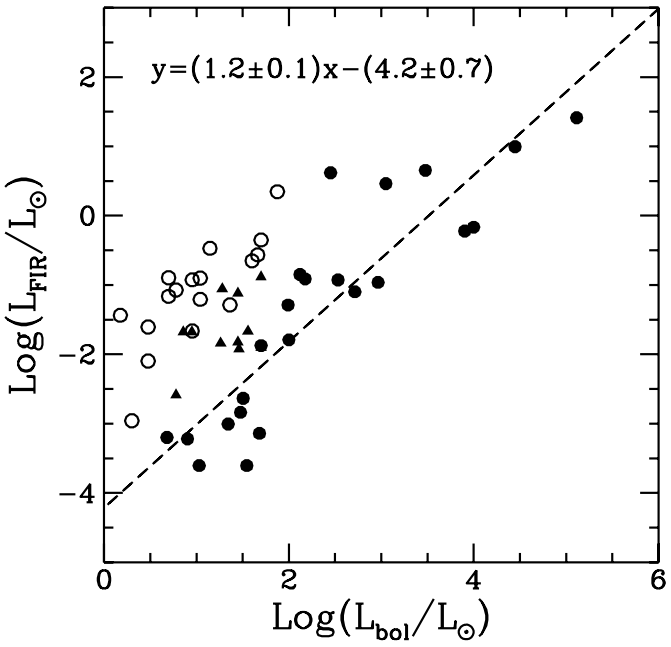

Fig. 7. Far IR lines luminosity *vs.* bolometric luminosity of the central star. The equation representing the best linear fit to the points (dashed line) is given in the upper part. HAEBE are represented as filled circles, while younger Class 0 and Class I objects (see text) are indicated with triangles and open circles, respectively.

and the column density required to have $\tau_{[\mathrm{OI}]\mathrm{lines}} \geq 1$, we obtain $l \simeq 2000$ AU, which seems an upper limit given the typical size of the clumps. Smaller values of l can be derived by assuming that only the 63 μm line is optically thick, while the 145 μm one is still optically thin. This situation obviously implies A_V values smaller than 27–18 mag. Therefore the low observed values of the 63/145 line ratio seem to be consistent with the presence of high column densities (roughly between 10 and 20 A_V) of a gas at 100–500 K, conditions which are not explored by the current models of PDR illuminated by interstellar radiation. In these models the observer is expected to see the illuminated emitting zone where temperatures between 500 and 100 K pertain to a gas with low optical depth ($A_V \approx 2$ mag). On the contrary, when the illuminating source (with an intensity likely stronger than that of the interstellar field) lies in the opposite side, the observer could see the emitting gas (at 100–500 K) at substantially higher column densities.

Finally we note that in the considered case (i.e. 63 μm line optically thick) the 63/145 ratio should not represent a suitable diagnostic tool to trace the density, but other line ratios, which include only the 145 μm transition, seem more appropriate to that scope. This is well demonstrated by the plot in Fig. 6, while we fail to obtain a meaningful matching between observations and models by using the 63 μm line in the same plot.

5.5. An evolutionary trend

Since our complete ISO-LWS sample (26 HAEBE out of 108) can be considered representative enough of the entire class, we have tried to derive some general trend to be compared with similar behaviours from classes of younger objects. We have computed the far IR luminosity (L_{FIR}) as due to all line emission contributions (fine structure line emission and total molecular cooling). In Fig. 7 these values are plotted as a function of the bolometric luminosity of the central object; the straight line, whose equation is given in the upper part of the Figure, represents the best linear fit to the points. We are aware of the distance bias built in the lum-lum plots which present (in the Log form) a linear correlation with unitary angular coefficient, thus we intend just to point out that the intercept on the y-axis is located at a L_{FIR} value of about 10^{-4}. A similar plot for the younger Class 0 objects (Nisini et al. 2002, here depicted as triangles) indicates $L_{\mathrm{FIR}} \simeq 10^{-2}$ as the intercept value. An intermediate value of 10^{-3} is attributable to the Class I objects (open circles), which are expected to be somehow younger than HAEBE and approaching to their evolutionary stage. The mechanisms invoked to account for the behaviour of the HAEBE stars and of the other objects are completely different: photodissociation due to FUV stellar photons for the former stars and shock excitation for the latter sources, where the L_{FIR} dependence on L_{bol} is related to the relationship between accretion rate ($\dot{M}_{\mathrm{acc}}$) and the mass loss rate ($\dot{M}_{\mathrm{out}}$). However it is worthwhile noting how L_{FIR} is a decreasing fraction of L_{bol} while the evolution goes on, although the different phases obey to different physical mechanisms. The conversion of the bolometric luminosity of the central object into far IR line cooling in the circumstellar envelope occurs at progressively lesser efficiency while time elapses. This fact extends to the far IR gas cooling the well consolidated statement according to which the relevance of the circumstellar vs. stellar properties diminishes during the pre-stellar evolution.

6. Conclusions

The main points of this work can be summarized as follows:

- The ISO-LWS archive has been systematically searched to obtain a complete far IR spectrophotometric survey of HAEBE stars: 15 new objects complement our original list of 11, leading to a final catalog of 26 objects, which represent about 25% of all the known HAEBE. Far IR spectra (from 45 to 200 μm at low resolution $\mathcal{R} \simeq 200$) of the new HAEBE stars have been analysed following the same approach as in our prior papers.
- [OI] 63 μm and [CII] 158 μm lines are observed in many of the investigated objects (with a detection rate of 73% and 85%, respectively), while the [OI] 145 μm is more difficultly detected (42%). Molecular lines in form of CO high-J rotational transitions are detected toward three sources and are associated to local density peaks (23%).
- A new class of ISO-LWS spectra of HAEBE has been put into evidence: that constitued by low luminosity objects ($L_{\rm bol} \lesssim 30\ L_{\odot}$) in whose spectra we do not detect any gas feature. In such cases, the weak [CII] 158 μm emission is likely a contribution due to a diffuse component not related with the star itself.
- Line intensities and intensity ratios have been compared with model predictions and we find that photodissociation by stellar photons, active in a clumpy medium, is the prevalent excitation mechanism.
- In a large number of cases the ratio [OI]63 μm /[OI]145 μm is anomalously less than expected. Optical depth effects are discussed as the most likely reason of these values: maybe some reconsideration of the PDR models toward more realistic morphologies of the emitting region could reconcile the observed discrepancy.
- An evolutionary trend is clearly recognizable in the ratio $L_{\rm FIR}/L_{\rm bol}$ between the luminosity due to all the line emission contributions and the bolometric luminosity of the central object. This ratio, which is about 10^{-4} for HAEBE, is smaller than that of younger objects, thus it decreases while the evolution goes on.
- This catalog serves as spectroscopic database for future space missions, when it will be possible to increase spatial resolution and sensitivity. The corresponding increase in the detection rate of both the [OI] 145 μm and molecular emission can be used for confirming the view presented here.

References

Benedettini, M., Nisini, B., Giannini, T., et al. 1998, A&A, 339, 159
Benedettini, M., Pezzuto, S., Giannini, T., et al. 2001, A&A, 379, 557
Bouwman, J., de Koter, A., van den Ancker, M. E., & Waters, L. B. F. M. 2000, A&A, 360, 213
Burton, M. G., Hollenbach, D. J., & Tielens, A. G. G. M. 1990, ApJ, 365, 620
Clegg, P. E., Ade, P. A. R., & Armand, C. 1996, A&A, 315, L38
Corporon, P., Ceccarelli, C., & Lagrange, A.-M. 1999, in The Universe as seen by ISO – ESA-SP 427, ed. P. Cox, & M. Kessler, 297
Creech-Eakman, M. J., Chiang, E. I., Joung, R. M. K., Blake, G. A., & van Dishoeck, E. F. 2002, A&A, 385, 546
Draine, B. T., Roberge, W. G., & Dalgarno, A. 1983, ApJ, 264, 485
Elia, D., Campeggio, L., Strafella, F., et al. 2002, A&A, submitted
Font, A. S., Mitchell, G. F., & Sandell, G. 2001, ApJ, 555, 950
Fuente, A., Martin-Pintado, J., Rodriguez-Fernández, N. J., Cernicharo, J., & Gerin, M. 2000, A&A, 354, 1053
Giannini, T., Lorenzetti, D., Tommasi, E., et al. 1999, A&A, 346, 617 (Paper II)
Harju, J., Haikala, L. K., Mattila, K., et al. 1993, A&A, 278, 569
Hollenbach, D., & McKee, C. F. 1989, ApJ, 342, 306
Hollenbach, D., Takahashi, T., & Tielens, A. G. G. M. 1991, ApJ, 377, 192
Kaufman, M. J., Wolfire, M. G., Hollenbach, D. J., & Luhman, M. L. 1999, ApJ, 527, 795
Kessler, M., Steinz, J. A., & Anderegg, M. E. 1996, A&A, 315, L27
Liseau, R., White, G., Larsson, B., et al. 1999, A&A, 344, 342
Lorenzetti, D., Tommasi, E., Giannini, T., et al. 1999, A&A, 346, 604 (Paper I)
Malfait, K., Waelkens, C., Waters, L. B. F. M., et al. 1998, A&A, 332, L25
Meeus, G., Waters, L. B. F. M., Bouwman, J., et al. 2001, A&A, 365, 476
Meyer, D. M., Jura, M., & Cardelli, J. A. 1998, ApJ, 493, 222
Molinari, S., Noriega-Crespo, A., & Spinoglio, L. 2001, ApJ, 547, 292
Nisini, B., Giannini, T., & Lorenzetti, D. 2002, ApJ, in press
Nisini, B., Lorenzetti, D., Cohen, M., et al. 1996, A&A, 315, L321
Palla, F., Testi, L., Hunter, T. R., et al. 1995, A&A, 293, 521
Petuchowsky, S. J., & Bennett, C. L. 1993, ApJ, 405, 591
Pezzuto, S., Strafella, F., & Lorenzetti, D. 1997, ApJ, 485, 290
Pilbratt, G. L. 2001, in The promise of the Herschel Space Observatory – ESA-SP 460, ed. G. L. Pilbratt, J. Cernicharo, A. M. Heras, T. Prusti, & R. Harris, 13
Saraceno, P., Nisini, B., Benedettini, M., et al. 1998, Proc. of Star Formation with the Infrared Space Observatory, ed. J. L. Yun, & R. Liseau, ASP Conf. Ser. 132, 233
Swinyard, B. M., Clegg, P. E., Ade, P. A. R., et al. 1996, A&A, 315, L43
Thé, P. S., de Winter, D., & Pérez, M. R. 1994, A&AS, 104, 315
Thi, W. F., van Dishoeck, E. F., Blake, G. A., et al. 2001, ApJ, 561, 1074
Tielens, A. G. G. M., & Hollenbach, D. 1985, ApJ, 291, 722
van den Ancker, M. E., Wesselius, P. R., & Tielens, A. G. G. M. 2000, A&A, 355, 194
van den Ancker, M. E., de Winter, D., & Tjin A Djie, H. R. E. 1998, A&A, 300, 145
Waelkens, C., Waters, L. B. F. M., de Graauw, M. S., et al. 1996, A&A, 315, L245
Watson, W. D. 1984, in Galactic and Extragalactic Infrared Spectroscopy, ed. M. F. Kessler, & J. P. Phillips (Dordrecht: Reidel), 195
Wesselius, P. R., van den Ancker, M. E., Young, E. T, et al. 1996, A&A, 315, L197